A Simplified Study of Storey Configurations

J. Carr

1) Introduction

This note compares various possible Km3NeT storey configurations by making simulation on a single storey and looking at the amount of light detected in the PMTs within a single storey. The simulation is made with the NESSY software which is described in ANTARES-SOFT-2007-011 as well as various ANTARES and Km3NeT presentations and conference proceedings. For the present simulation light is generated from electro-magnetic showers as well as the Cherenkov process but the light scattering option is turned off.

The quantity used for the comparison is the efficiency that photons are detected on the storey from tracks generated on a cylindrical can relatively close to the storey. The method uses the efficiency for detecting one photon; for detecting two photons and for a coincidence of at least one photon on at least two PMTs in the storey. The effect of different can sizes will be presented. The efficiencies at different energies will be shown and for one storey configuration the effect of changing some geometric parameters will be given.

The initial motivation for this study was to optimise the "NuOne" detector configurations but comparisons are made with ANTARES, NEMO and "MultiPMT" configurations.

2) Optimisation Philosophy

The objective of this note is to contribute to the choice of the full Km3NeT detector geometry. The philosophy is that the choices must start with the PMT type and the PMT configuration inside the storey. The single storey efficiencies will be used to give indications on the choice of storey spacing as well as complete detection unit separations.

It is well known that the optimum geometry depends on the energy range of interest and this energy range depends on the science objectives of the Neutrino Telescope. In this note the assumption is that the main science goal is neutrino astronomy and for this reason most simulations will be performed with a unique energy of 10 TeV although comparisons will be made with other energies.

Further, a choice must be made on the zenith angle range of tracks for the optimisation. Depending on the depth of the detector neutrinos can be separated from muons up to 10-15° above the horizontal. In order to make this separation it is important to have good resolution on downward going muons at higher angles than these values to avoid contamination due to measurement errors. This note uses the photon detection efficiency for tracks from the full upward angular ranges and for the downward hemisphere up to 30° above the horizontal.

It is emphasised that the full detector cost is the essential element in the optimisation and that "Science per Euro" is the criterion which must be employed. For a neutrino telescope, as for any tracking detector, the ideal distribution of detector elements is homogeneous throughout the volume. Since the major cost in the telescope is in fact not the detector elements but the structures and connections to hold these elements (e.g. The PMT cost in ANTARES was 5% of the total) a compromise between the ideal tracking configuration and the cost is necessary. It is this compromise which must be the goal of the optimisation.

3) Storey configurations considered

Four storey configurations will be considered the NuOne configuration described in the recent document presented to the Km3NeT PCC; the MultPMT configuration discussed on many occasions and detailed in another recent presentation to the PCC; the standard ANTARES configuration and the NEMO configuration being used for the Phase II Tower.

Figure 1 illustrates the four configurations and Table 1 gives some details of PMT sizes and geometrical parameters.

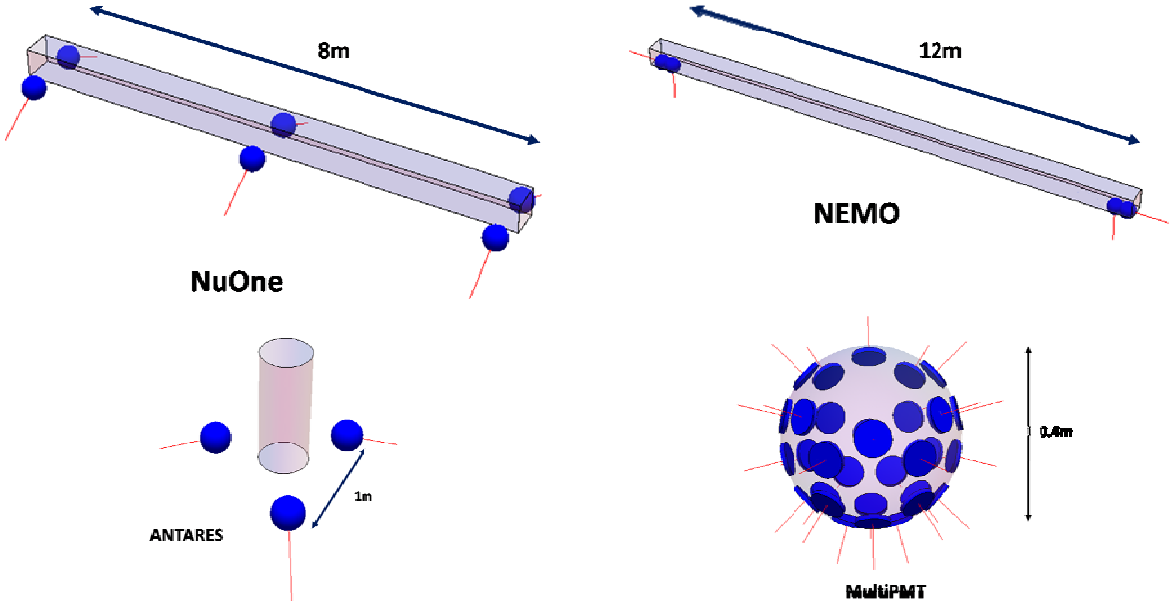

Figure 1. The four storey configurations simulated: NuOne; NEMO; ANTARES; MultiPMT

Detector Name	PMT /storey	PMT orientation	PMT size	Quantum efficiency	OM transmission	area per storey	PMT angular acceptance
NuOne	6	60°	8"	35%	0.98	0.067 m^2	0.77
NEMO	4	0°, 90°	10"	23%	0.94	0.044 m^2	0.77
ANTARES	3	45°	10"	23%	0.94	0.033 m^2	0.77
MultiPMT	31	0°-124°	3"	42%	0.97	0.057 m^2	0.50

Table 1. Details of the four storey configurations considered in this note. "OM transmission" is a factor which takes into account absorption in the glass, gel and mu-metal shield. "Area per storey" is the total effective area taking into account the quantum efficiency and transmission coefficient for tracks with normal incidence to the PMT; it is given only as an indication the simulation takes into account all effects. "PMT angular acceptance" is the integral over cosθ of the OM angular acceptance functions described in section 4.

4) <u>OM angular acceptance</u>

For the simulation, an angular acceptance of the optical module is necessary. For the ANTARES OM, much effort has gone into obtaining this angular acceptance but uncertainties remain. The function used is the "Genova with cut off 0.8":

$F(\cos\theta)=0.34888-0.54723\cos\theta+0.062665\cos^2\theta+0.035784\cos^3\theta+0.076725\cos^4\theta$.

For the multPMT configuration, as yet no measurements have been made and an estimation has been made by Jean-Pierre Ernenwein with GEANT4 which gives the form for $\cos\theta>0.25$:

$F(\cos\theta)=(0.0020-0.022\cos\theta+0.054\cos^2\theta+0.071\cos^3\theta+0.033\cos^4\theta)/(0.0020+0.022+0.054-0.071+0.033)$.

Figure 2 shows these angular acceptance functions and the integrals over cos θ are given in table 1.

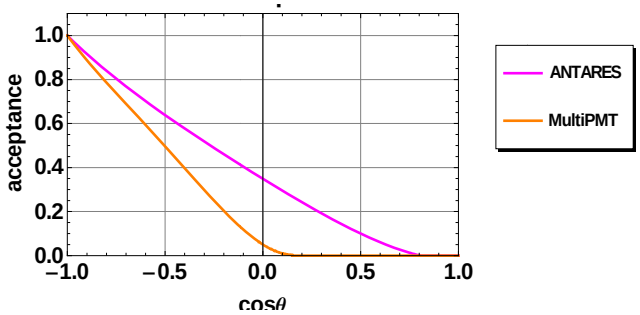

Figure 2. OM angular acceptances used, where θ is the angle of incidence of the light to the OM

5) Light acceptance of storey configuration

For the four storey configurations, Figure 3 shows contour plots indicating the regions in space for which on average the given number of photons are detected.

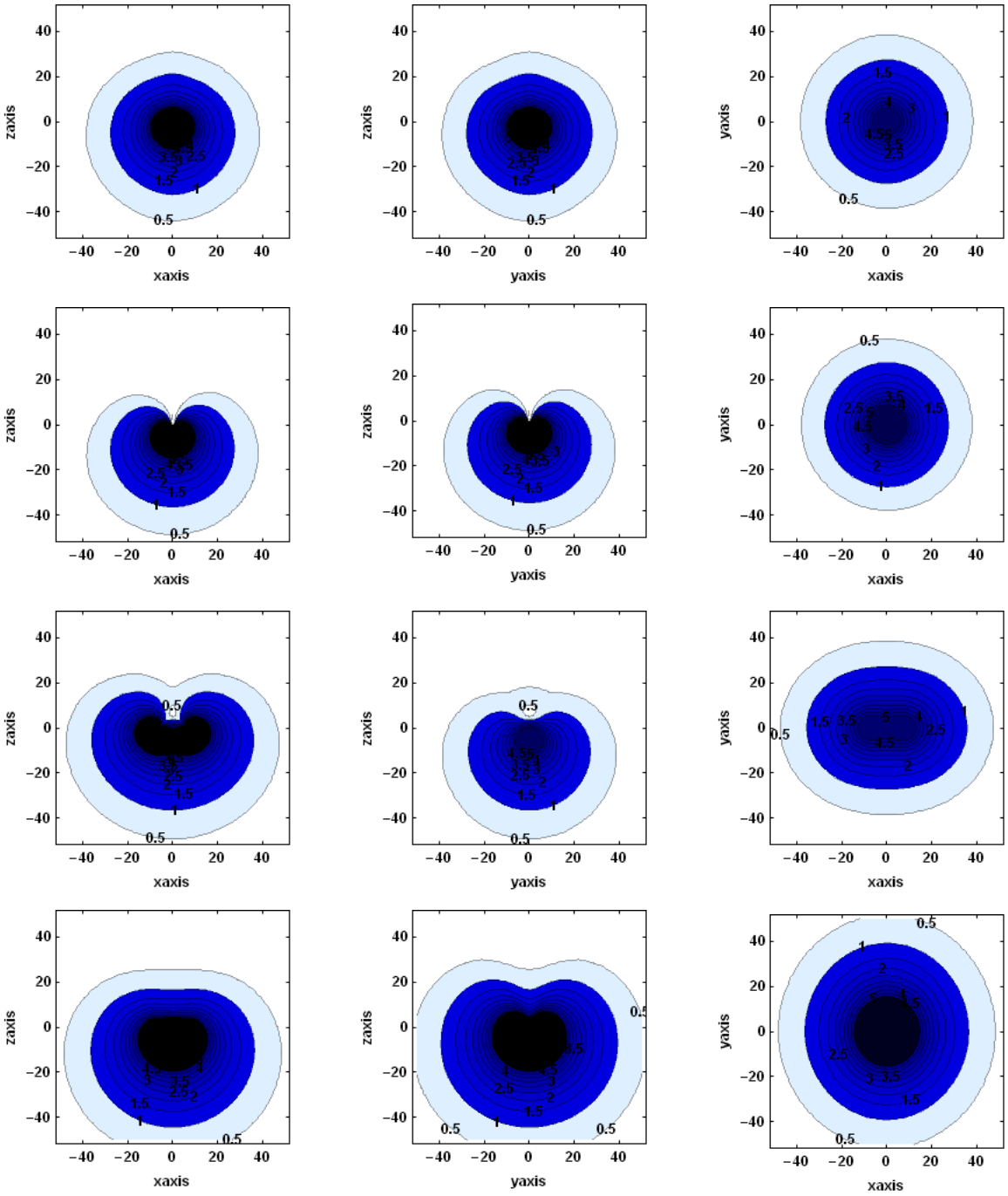

Figure 3. Density of detected photon field. The contours start for 0.5 photons with intervals of 0.5 photons. The four rows are for storeys of : MultiPMT, ANTARES,NEMO and NUONE from top to bottom respectively. The centre of the storey is at (0,0,0) and the bars of NuOne and NEMO are extended in the x dimension. The left column is the (x,z) plane for y=0; the middle column is the (y,z) plane for x=0 and the right column is the (x,y) for for z=-10m. The axes scales are in m.

As can be expected the storeys with larger effective photocathode detection area cover a larger volume. All configurations have roughly hemispherical coverage in the downward looking hemisphere. The MultiPMT configuration has the largest coverage in the upward hemisphere. For the two bar configuration NuOne and NEMO the full bar length is respectively 8m and 12m in the x

dimension. For NEMO the contour plot is elongated in the x dimension while for NuOne the distribution is more symmetric with a slight broadening in the y dimension corresponding to the orientation of the PMT axes.

6) Correction for biofouling / sedimentation

For the simulations in this note a small modification to the NESSY code has been made to take into account the light losses due to sedimentation and biofouling on the glass surfaces. Since this correction is small approximations have been made in the implementation.

The ANTARES site exploration results show a loss of light transmission though the sphere due to biofouling and sedimentation on the surface. The magnitude of the transmission loss depends critically on how close to horizontal is the glass surface. The extreme case is the north pole of the sphere where the transmission coefficient is T=0.4 after 100 days. At surfaces close to the vertical the loss is very low T~0.99. For intermediate values fluctuate around 0.8-0.9 with time and approach a constant value due to a washing effect in the sea current. Table 2 estimates the transmission coefficient for different points on the sphere, extrapolating to one year after deployment.

Angle of surface to horizontal	0°	30°	60°	70°	90°
Transmission coefficient	0	0.9	0.9	0.94	0.99

Table 2. Transmission due to biofouling and sedimentation estimated from ANTARES site measurements.

Figure 4 illustrates the angle between vertically downward going light and the glass surface for three of the optical modules simulated in this note. The figure indicates the maximum angle and for each case there would in reality be a range of angles. These angles are all in the range of 40-50° for which the transmission coefficient can be seen to be ~0.9 from table 2. In the simulation the effect is taken into account by applying a transmission coefficient as a function of the direction of the light relative to the vertical as given in figure 5. This effect reduces all efficiencies discussed in this note by less than 1%, as shown in figure 15. Even tiny, the correction is retained for completeness.

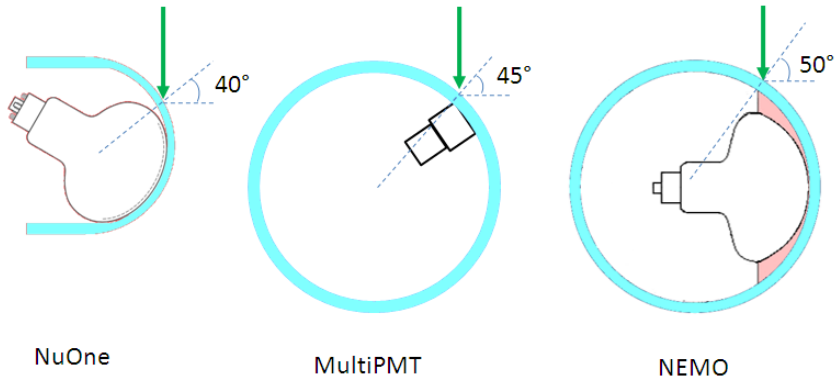

Figure 4. Geometrical indication of maximum angles of incidence of downward going vertical light to glass surface in order to estimate the worst case situation for light loss from biofouling / sedimentation.

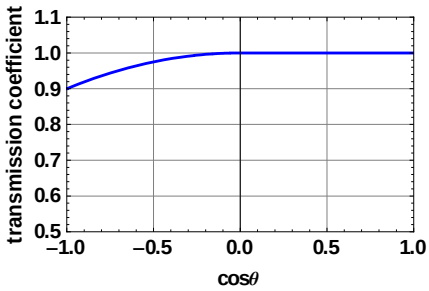

Figure 5. Correction for transmission losses due to biofouling, θ is the angle of the light relative to the vertical.

7) Rationale of Method

As stated in the introduction, the method adopted is to generate tracks on a can around the single storey and to define efficiencies which are the proportion of generated tracks to give photons and coincidences in the storey. The can size is thought of as having height equal to the spacing of storeys in the detection units and radius equal to half the detection unit spacing. Vertically the cans start at the storey, defining z=0, and extend downwards to the z coordinate of the next storey. With this the full space of the detector will be covered with can volume except for a tiny space as indicated in Figure 6. In this example the detector units are distributed on a hexagonal lattice as this minimises the uncovered spaces in this method but also minimises the distance from any point in the detector to a detection units and so is thought of as the optimal detection arrangement.

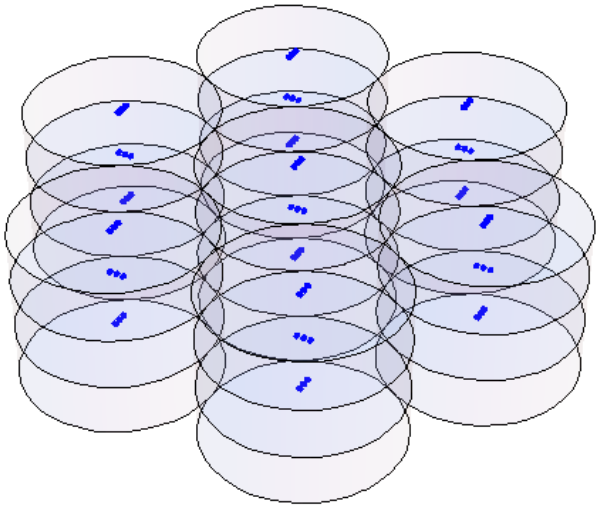

Figure 6. Space covered by the generation cans in a complete detector. The detection units are spaced by twice the can radius in a hexagonal lattice. The can height is equal to the storey spacing and covers just the space below the storey.

The method is further illustrated in figure 7 which plots the points where coincidences are record in space around the storey. The can dimensions are indicated, which in this example the can has height 30m and radius 55m and the tracks have energy 10 TeV. These parameters are the defaults and will be used for all plots without differing indications.

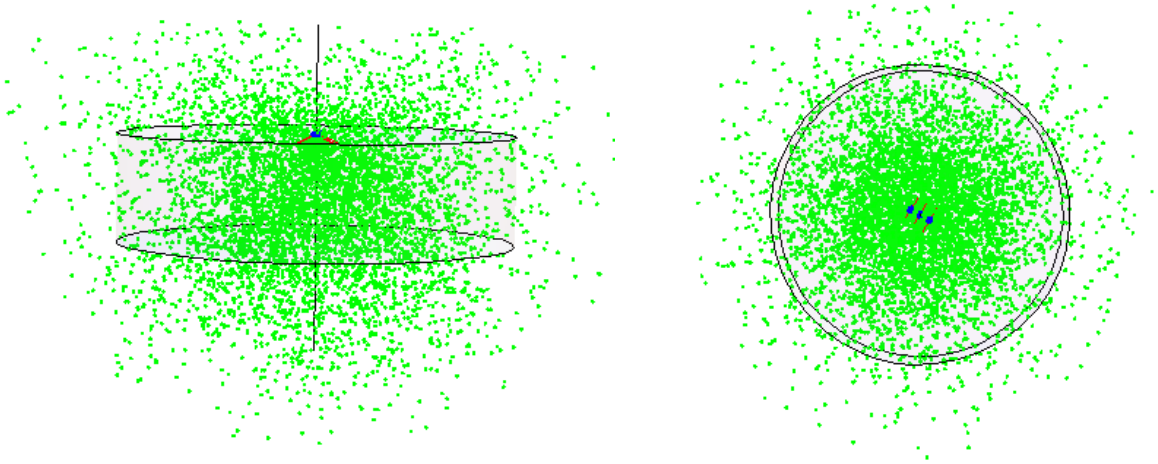

Figure 7. Space distribution of light emission points on track when there is a coincidence of two PMTs in the NuOne detector storey. The cylinder is the generation can through which the generated tracks can pass; as is seen it is possible that the light emission points are on the track outside the can.

8) Coincidences in storey

This note evaluates the efficiency of the storeys using three efficiencies. The first efficiency is the proportion of events with at least one photon, i.e. one photo-electron, detected in any PMT in the storey. The second efficiency is that to detect photon is any PMT and the third efficiency is to have at least two photons in different PMTs For events with a coincidence figure 8 shows the time difference between each individual hit and the mean time of all hits in the storey. These plots are for only geometrical delays in the light paths and do not include PMT time resolutions. The definition of coincidence efficiency has no time window limit. It is seen that for all storey configurations the time differences are largely within a window ±50ns.

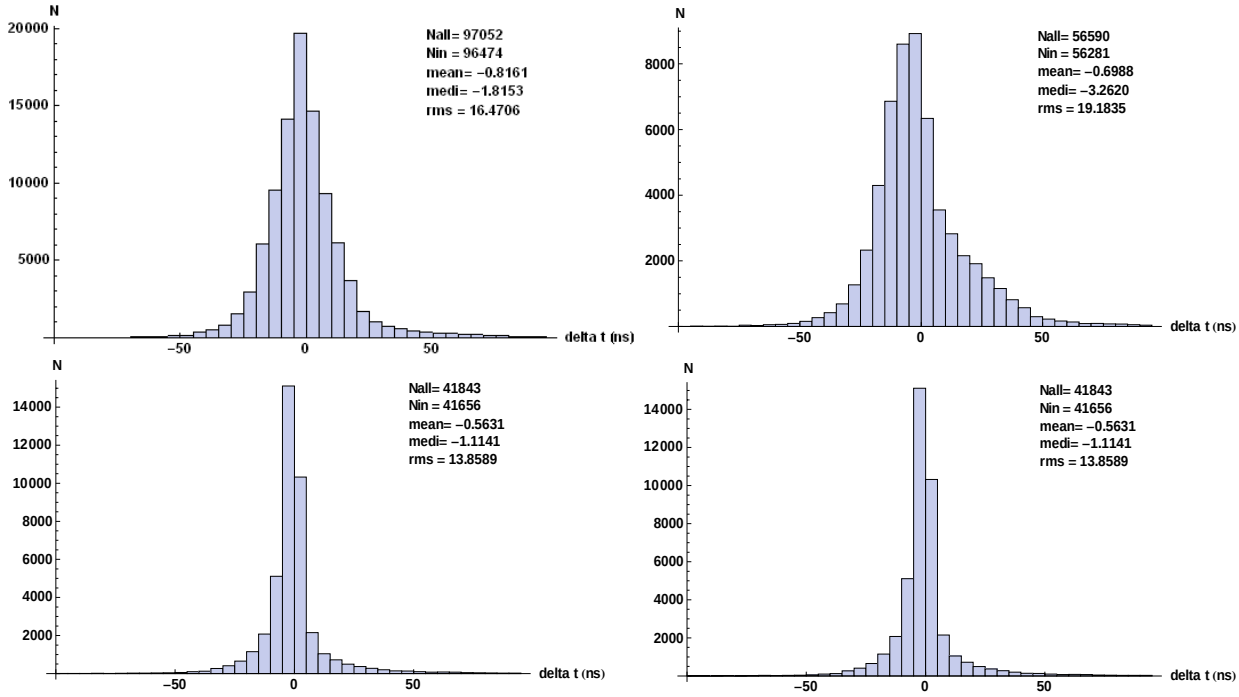

Figure 8. Time difference between coincident hits in storey. For the four configurations(top NuOne, NEMO, bottom ANTARES, MultiPMT) the histograms show for events where there are at least two hits in different PMT in the storey, the difference between the mean time and each individual hit.

The different storey configurations have somewhat different ratios between these three efficiencies as shown in table 3. In particular the storeys with more individual PMTs have a higher proportion of coincidences as would be expected. However, even for ANTARES 81% of events with two photons are coincidences. This ratio increases to 98% for the MultiPMT option and 92% for NuOne. From this it could be concluded that the importance of resolving one and two photons within the same PMT is not paramount and would only give gains in trigger efficiencies ~ 10%.

		NuOne	NEMO	multiPMT	ANTARES
Efficiency ratio	two/one photon	0,66	0,61	0,58	0,58
	coincidence/two photon	0,92	0,84	0,98	0,81

Table 3. The ratio of efficiencies as indicated. The table is for track energy 10 TeV, $-0.5<\cos\theta<1.0$ and the default can size.

9) Zenith angle and Azimuthal angle dependence

Figure 9 shows the efficiency for a coincidence in the storey as a function of the cosine of the zenith angle. It can be seen that the ANTARES, NEMO and NuOne configurations have efficiencies which are significantly higher for upward going tracks while the MultiPMT is much more isotropic.

This difference is clearly due to the differences of pmt orientations. Figure 10 shows the corresponding plot as a function of azimuthal angle, indicating that all configurations are close to isotropic in azimuth.

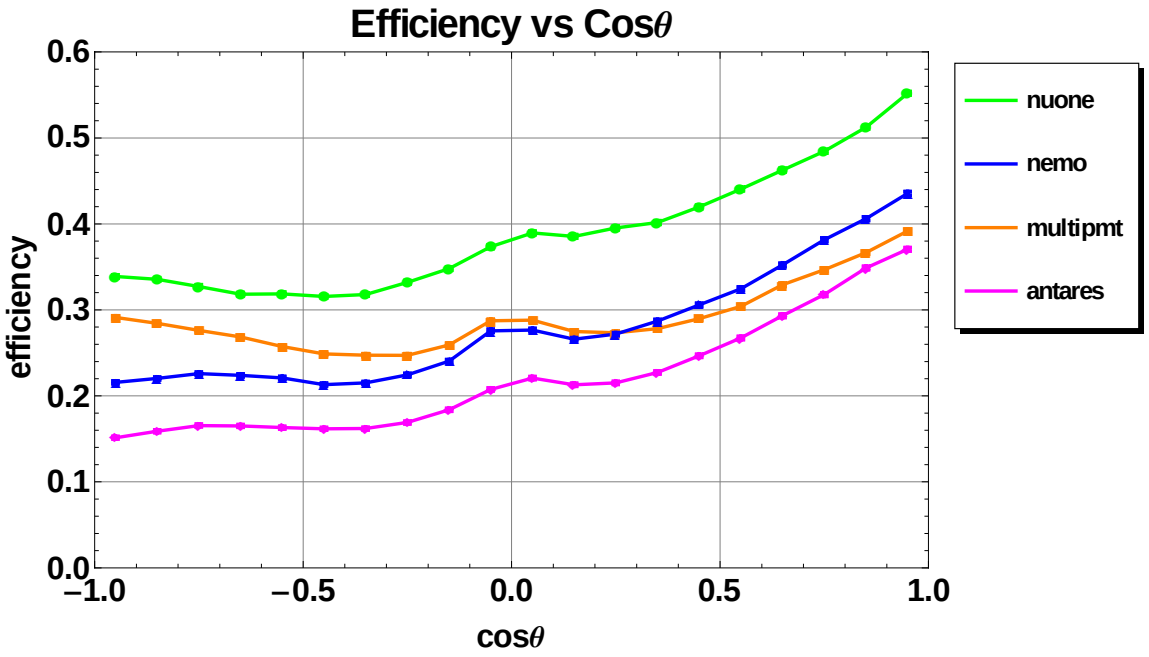

Figure 9. Efficiency for a coincidence of two PMT with hits on the storey as a function of the zenith angle for track energy 10 TeV and the default can size. The statistical error bars are plotted.

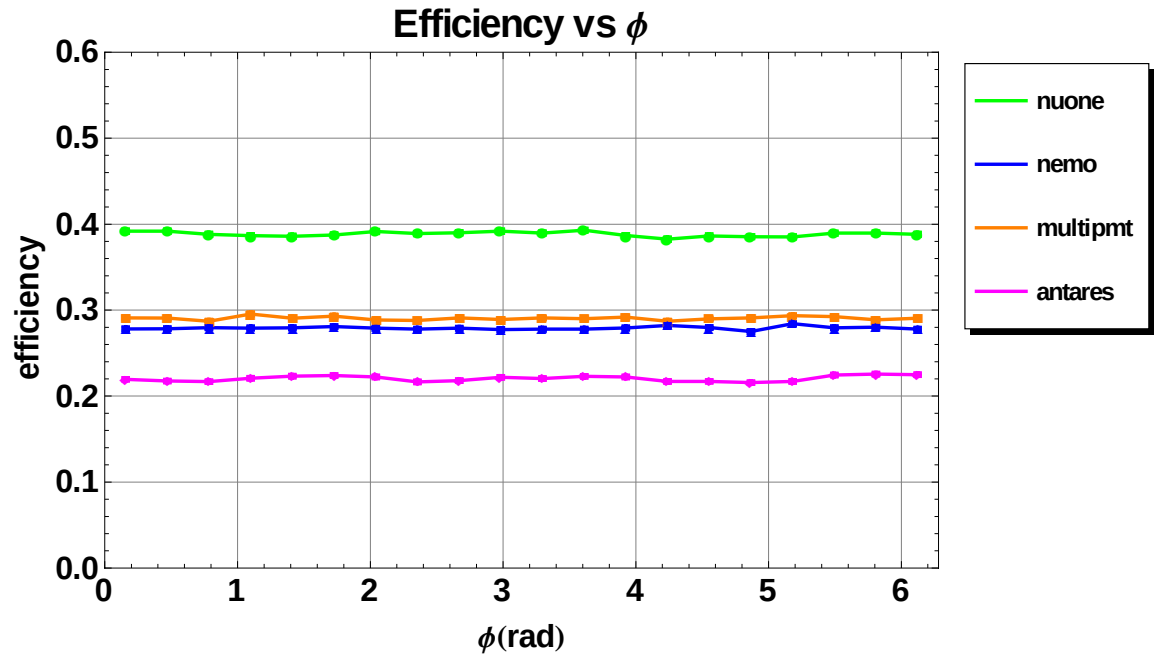

Figure 10. Efficiency for a coincidence of two PMT with hits on the storey as a function of the azimuth angle for track energy 10 TeV integrating over the full zenith angle range $-1.0<\cos\theta<1.0$.

As discussed earlier the quantity in general used for evaluation in this note is the efficiency in the range $-0.5<\cos\theta<1.0$, hence somewhat disfavouring the MultiPMT option which has relatively higher efficiency in the downward direction.

10) Optimisation of NuOne configuration

This section shows details of the NuOne configuration in order to explore the optimisation of the geometry. Figure 11 shows the energy dependence of the three efficiencies defined. At high energies all efficiencies tend towards one and become similar. The ratio two/one efficiency goes from 60% at 1 TeV to 82% at 1 PeV while the ratio coincidences/two photon efficiencies goes from 89% to 96%.

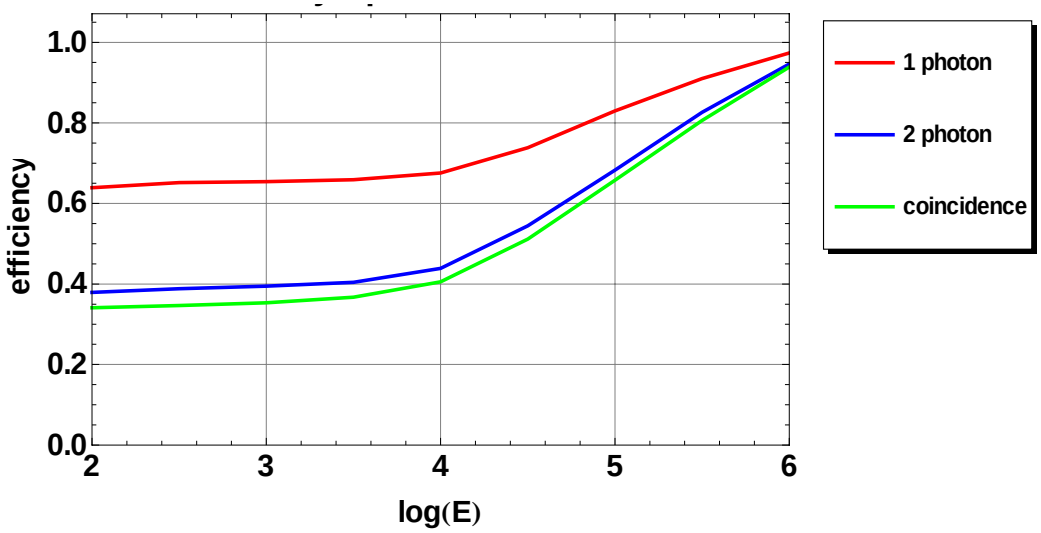

Figure 11. Efficiency to detect one, two photons and coincidence in a NuOne storey as a function track energy for the zenith angle range $-0.5<\cos\theta<1.0$.

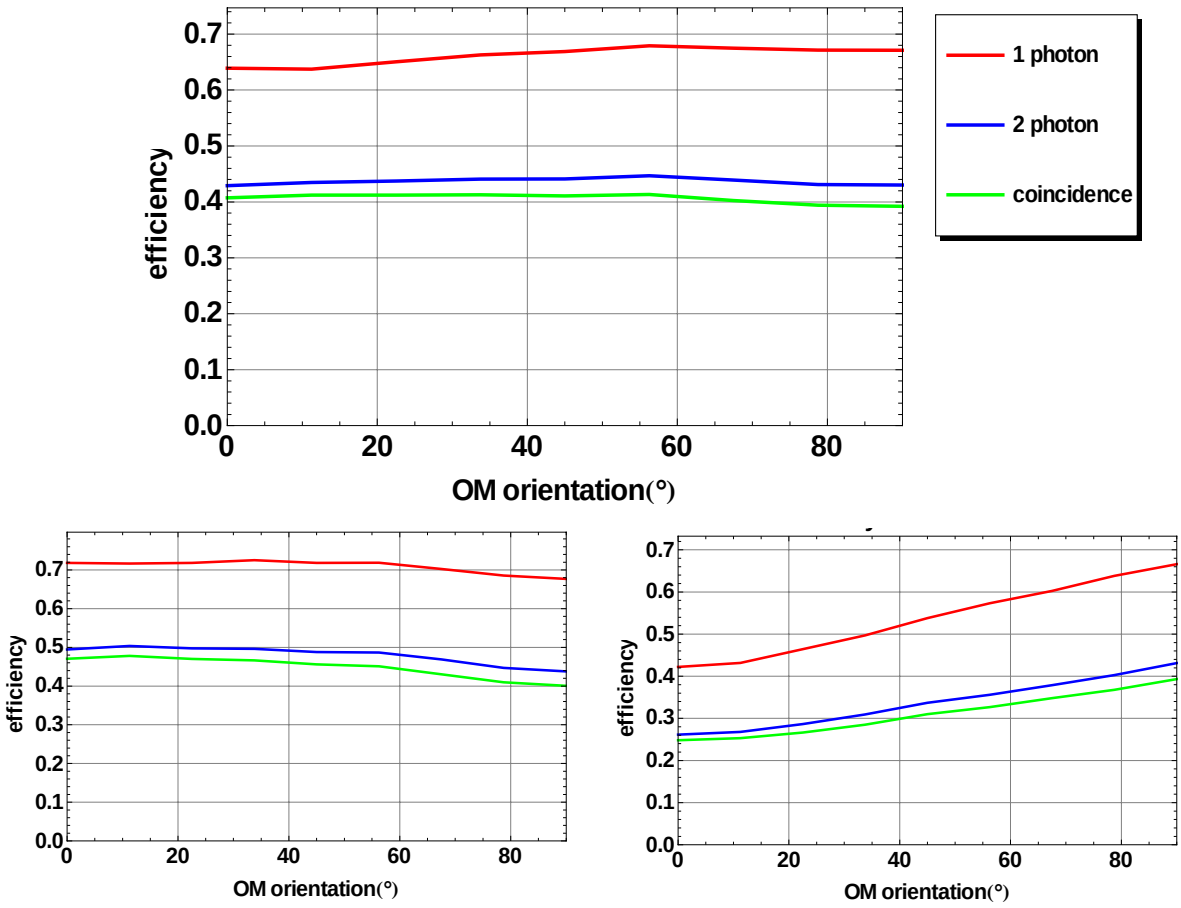

Figure 12. Efficiency for one, two photons and coincidences with a NuOne storey changing the PMT orientation from the default 60° to the downward vertical in the range 0° (vertical) to 90° (horizontal). The upper plot is for the zenith angle range $-0.5<\cos\theta<1.0$ and the lower plot on left for $0<\cos\theta<1$ and right $-1<\cos\theta< 0$.

For the NuOne storey the default PMT axis orientation is so far taken to be 60° to the downward going vertical. Figure 12 explores the change in efficiency by changing this orientation between all 6 PMTs vertical and all 6 horizontal. For only upward going tracks, $0<\cos\theta<1$, the optimal orientation is for small angles to the vertical, whereas for downward going tracks, $-1<\cos\theta<0$, the optimal is for a horizontal orientation. For the defaults zenith angle ranges defined, $-0.5<\cos\theta<1$, the efficiencies are rather flat rising a little toward 60° and then falling slightly. Hence, choosing the value of 60° seems to be a reasonably optimal.

The effect of changing the separation of the PMTs in the NuOne configuration, the "bar length" is shown in Figure 13. The variation of efficiency with bar length is clearly tiny, the gain in efficiency for bar length must be due to reconstruction effects.

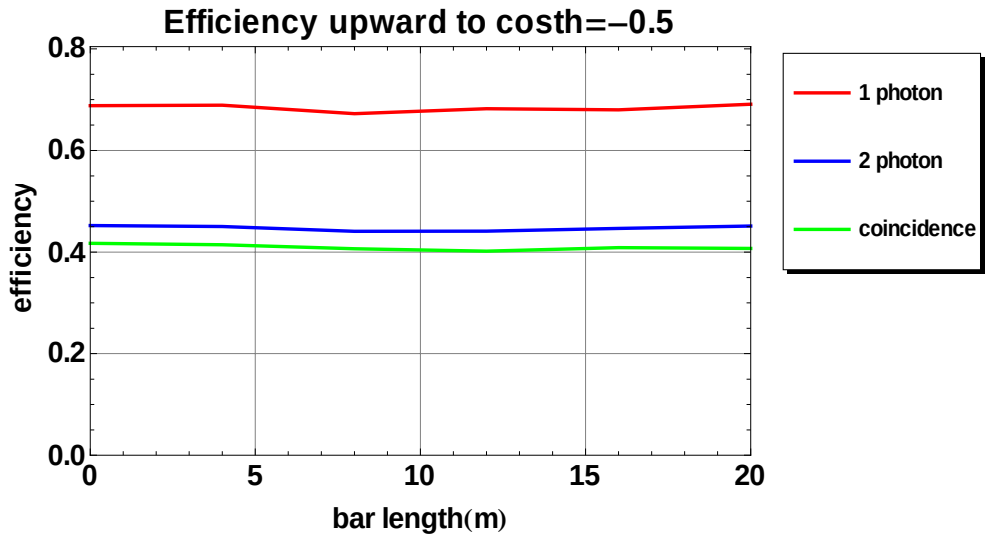

Figure 13. Efficiency to detect one, two photons and coincidence in a NuOne storey with different PMT separation by changing the bar length relative to the default 8m. The plot is for the zenith angle range $-0.5<\cos\theta<1.0$.

11) Dependence on parameters

In this section the dependence of the efficiency on certain parameters in the simulation is explored. Firstly, in figure 14 a simulation for the MultPMT storey is shown with and without the correction for light transmission loss due to sedimentation described in section 6. As already stated the effect is tiny and only significant for downward tracks as expected.

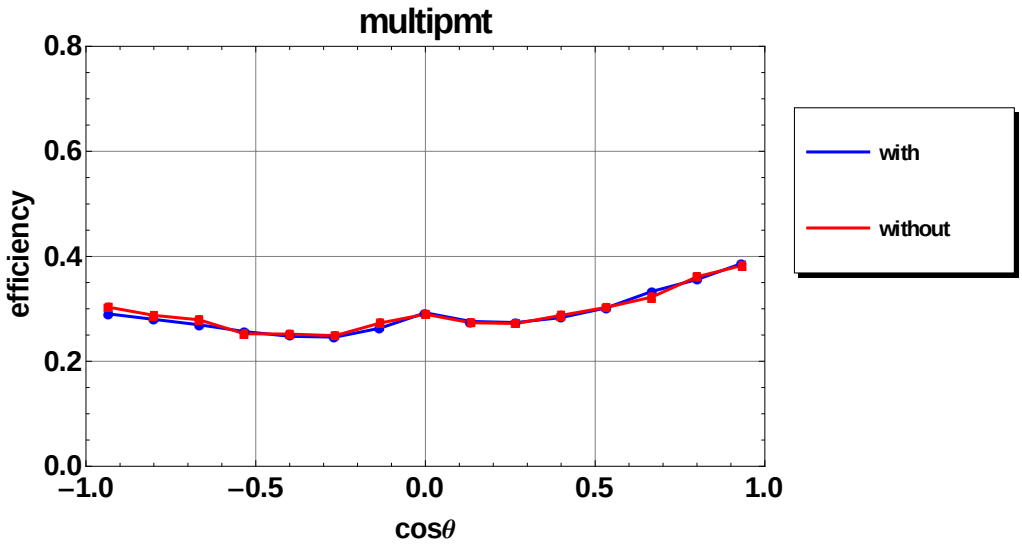

Figure 14. Efficiency for a coincidence in MultiPMT storeys with and without the correction for sedimentation.

Figure 15 shows the effect of changing the OM acceptance by imposing an artificial cut-off in the acceptance at cosθ=0.65 in the function shown in figure 2. The effect is small for both the NuOne and ANTARES storeys which could be expected since the difference in the integral of the angular acceptance functions is only 0.4%.

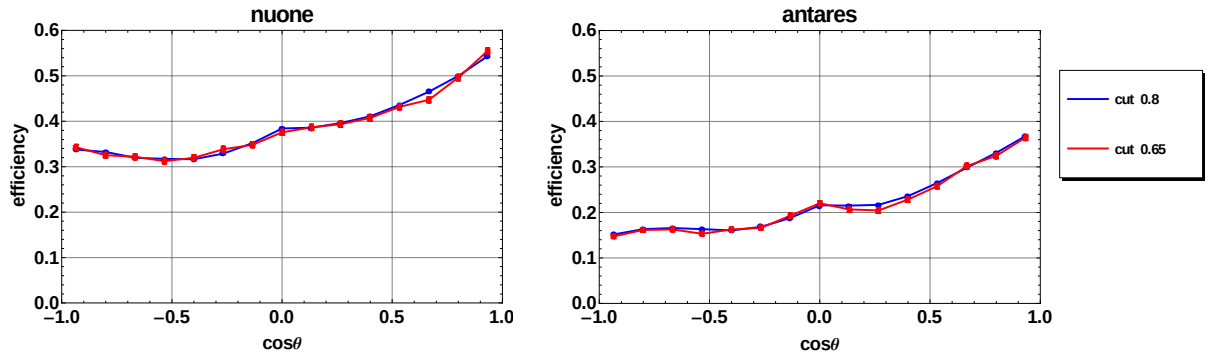

Figure 15. Efficiency for a coincidence in NuOne and ANTARES storeys with different PMT angular acceptance between the standard ANTARES OM acceptance shown in figure 2 which has a cut-off at cosθ=0.8 and one with a cut-off at 0.65.

The effect of changing the light absorption length is significant as can be seen in figure 16.

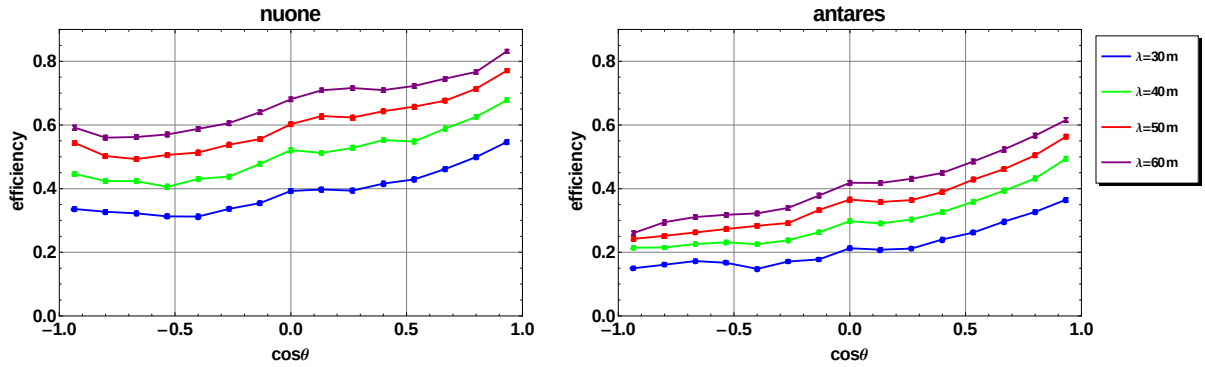

Figure 16. Efficiency for a coincidence in NuOne and ANTARES storeys with different light absorption lengths, changing from the default λ=30m to λ=40, 50, 60m.

12) Efficiency comparisons for the four storey configurations

Table 4 summarizes the efficiencies with the default parameter values for the simulation. The table contains rows where the efficiencies are normalized in order to more easily compare the configurations. The efficiencies normalized to ANTARES make clear that the MultiPMT configuration is 5% more efficient than ANTARES for one and two photon efficiencies, but 27% more efficient for coincidences due to the fine granularity; it can be seen that for the MultiPMT option 98% of two photon events are coincidences compared to 81% for ANTARES. The NuOne option has the highest efficiencies and 92% of two photon events as coincidences because of the 6 PMT per storeys. The rows with efficiencies normalized to total effective photocathode area indicates normalized values always higher for ANTARES, this being because in dense storeys photocathode area is “wasted” in the overlap when only low numbers of photons are required. This matches with the statement earlier that the ideal tracking detector spreads uniformly the detection elements.

		NuOne	NEMO	multiPMT	ANTARES
total effective photocathode area (m^2)		0,067	0,044	0,057	0,033
Efficiency	one photon	0,678	0,590	0,526	0,508
	two photon	0,445	0,361	0,303	0,294
	coincidence	0,409	0,305	0,296	0,237
Efficiency relative to ANTARES	one photon	1,34	1,16	1,04	1,00
	two photon	1,51	1,23	1,03	1,00
	coincidence	1,72	1,28	1,25	1,00
Efficiency per area 0,033 m^2	one photon	0,33	0,44	0,30	0,51
	two photon	0,22	0,27	0,17	0,29
	coincidence	0,20	0,23	0,17	0,24

Table 4. Efficiency values for the detection of one photon, two photons and a coincidence in each of the storey configurations considered. The top set of values give the absolute values, the second set relative to the ANTARES efficiency and the third set normalised to the effective photocathode area for the complete storey. The table is for track energy 10 TeV, $-0.5<\cos\theta<1.0$ and the default can size. The statistical errors in the efficiencies are ~0.4%.

Figure 17 shows the dependence of the efficiency on the track energy. For this plot it is the efficiency to detect two photons in a storey in contrast with figure 8 which shows the efficiency for a coincidence. It can be seen that the two photon efficiencies approach 1 at the highest energy and that as energy increases the difference between the configurations diminishes. At energies of 1 TeV and below the relative two photon efficiencies are NuOne: NEMO: MultiPMT: ANTARES = 1.75:1.29:1.03:1, more favourable for the NuOne configuration.

Figure 18 shows the change of the efficiency with the generation can radius. As indicated in Figure 6 the can radius is considered to be half the detector line separation and so this figure can be interpreted as efficiency as a function of detector unit separation. All configurations are seen to have similar dependence on the can radius and for all for larger can radii, corresponding to larger line spacing the efficiency diminish indicating dead zones in the detector

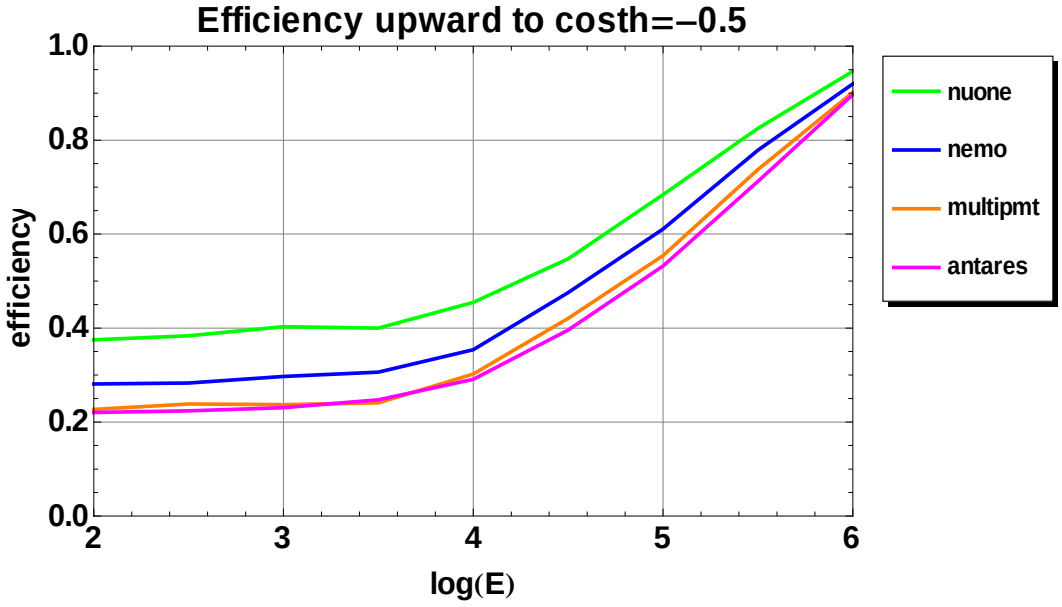

Figure 17. Efficiency to detect two photons in a storey as a function track energy for the zenith angle range $-0.5<\cos\theta<1.0$ with the default can radius of 55m. (NB. This plot shows the two photon efficiency while figures 9 and 10 show the coincidence efficiency).

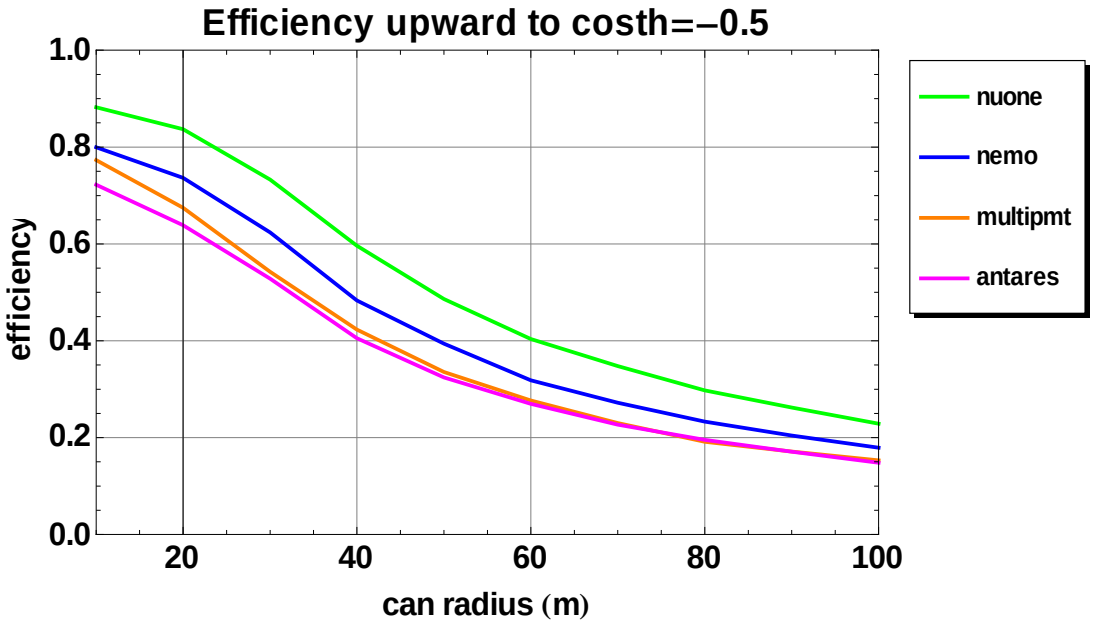

Figure 18. Efficiency to detect two photons in a storey as a function of can radius, for track energy 10 TeV and for the zenith angle range $-0.5<\cos\theta<1.0$.

13) Cost comparison of configurations

The previous section presented efficiency comparisons of storeys configurations witch different effective PMT area. Unsurprisingly storeys with higher effective area have higher efficiency. To make a real comparison a different detector layout configuration must be considered and for this a comparison is made using detector units with different numbers of storeys such that the total effective area per detection unit is constant.

As already emphasised, any optimisation must include a cost evaluation. For the note the cost model of Stéphan Beurthey ref[x] is used. In this model a detection unit with 40 storeys with 3 ANTARES OM separated by 15m is compared with a detection unit of 20 storeys with 6 ANTARES OM, giving a detection unit with the same number of PMT. The result is that the 40 storey model is a factor 1.31 more expensive. From table 3 one can quantify the detector efficiency ratio from the efficiency normalised to photocathode area. This then gives detector unit with 40 storeys more efficiency a factor 1.17 for coincidences, 1.34 for two photons and 1.51 for single photons. So based on coincidences the detector with fewer storeys is optimal, but based on single photons the inverse!

14) Discussion

The final choices for Km3Net geometry must be based on full MC simulation of the effective neutrino area after reconstruction and with appropriate event quality cuts. A similar complete simulation and reconstruction of atmospheric muon background is required to demonstrate that the quality cuts are adequate to give the necessary background reduction. The results of the simulations in this note are an attempt to reduce the parameter space of geometries which must be tested with the full time consuming procedure.

The conclusions which are clear from this study are those within the same configuration, while the comparison of configuration is more contestable. The advantage of the method has been that high statistics with many variations of parameters are possible and so the comparisons are definitely statistically significant. It is clear, from figure3 and figure8, that all storeys have complete azimuthal coverage; in particular the bar configurations, NuOne and NEMO, have no holes in ϕ and are rather symmetric always having higher or similar acceptances than the local configurations ANTARES and MultiPMT. The orientation of the PMT for the NuOne configuration is not critical and the choice of 60° is reasonable.

Between storey configurations in absolute values the NuOne configuration always has better efficiency. However, when normalizing to the same total effective photocathode areas the ANTARES configuration has more efficiency per m^2 than the other configuration. This goes in the sense that the absolute ideal configuration has the photocathode area spread as uniformly as possible in space. Cost configurations are needed to go away from the ideal to find the optimum cost wise. A rapid cost evaluation has been used which indicates that the NuOne configuration is better than ANTARES if the coincidence efficiency is used as the criterion. More detailed simulations are required with a full detector simulation and reconstruction as well as complete cost evaluations to be certain of this conclusion.

15) Conclusions

For the NuOne storey configuration:

- The azimuthal coverage is uniform
- The PMT orientation is not critical and 60° to the vertical is reasonably optimal
- Coincidences are 92% of all events with at least two photons
- Transmission losses due to sedimentation are negligible
- A configuration with more PMTs per storey and fewer storeys is cost effective

It is felt that an objective choice between detector configurations can only be made using full cost estimates. It is likely that many configurations are similar from the pure performance point of view and the “Science per euro” criterion must be the basis to choose.